Journal of Hazardous Materials 461 (2024) 132559

Contents lists available at ScienceDirect

Journal of Hazardous Materials

journal homepage: www.elsevier.com/locate/jhazmat

Environmental forensics approach to source investigation in a mercury contaminated river: Insights from mercury stable isotopes

Young Gwang Kim [a], Sae Yun Kwon [a,b,*], Spencer J. Washburn [c], Yongseok Hong [d], Seung Hee Han [e], Mikyung Lee [f], Ji Hyoung Park [f]

[a] Division of Environmental Science and Engineering, Pohang University of Science and Technology, 77 Cheongam-Ro, Nam-Gu, Pohang 37673, South Korea
[b] Institute for Convergence Research and Education in Advanced Technology, Yonsei University, 85 Songdogwahak-Ro, Yeonsu-Gu, Incheon 21983, South Korea
[c] Geosyntec Consultants, Inc., 100 Washington Ave. S, Suite 1590, Minneapolis, MN 55401, USA
[d] Department of Environmental Engineering, Korea University Sejong Campus, 2511 Sejong-Ro, Sejong City 30019, South Korea
[e] School of Earth Sciences and Environmental Engineering, Gwangju Institute of Science and Technology (GIST), 123 Cheomdangwagi-Ro, Buk-Gu, Gwangju 61005, South Korea
[f] Water Environmental Engineering Research Division, National Institute of Environmental Research, 42 Hwangyeong-Ro, Seo-Gu, Incheon 22689, South Korea

HIGHLIGHTS

- Environmental forensics approach was applied for Hg isotope source tracing.
- Four plausible contamination scenarios were assessed in a Hg-contaminated river.
- Hg isotopes confirm that historical collapse of a landfill is the dominant Hg source.
- Present Hg release is also possible given the elevated wastewater Hg level.
- Landfill collapse and wastewater contribute 61 % and 22 % to the Hg-contaminated river.

GRAPHICAL ABSTRACT

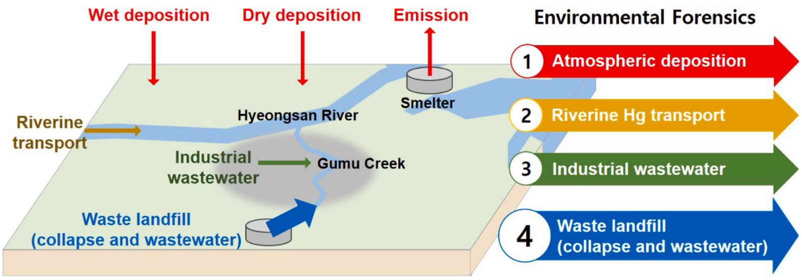

ARTICLE INFO

Editor: <Edward Burton>

Keywords:
Source tracing
Mercury contamination
Isotope fingerprinting
Wastewater
Sediment

ABSTRACT

Environmental forensics approach was applied to assess the efficacy of mercury (Hg) stable isotopes for source screening and decision-making in the Hyeongsan River, South Korea. Four Hg contamination scenarios were identified– atmospheric Hg emissions from a steel manufacturing industry, upstream riverine Hg transport, and industrial Hg releases and historical landfill collapse from Gumu Creek. The absence of significant Hg isotope difference between the Hyeongsan River sediments (δ^{202}Hg; −0.46 ± 0.17‰, Δ^{199}Hg; −0.04 ± 0.06‰) and the Gumu Creek sediment (δ^{202}Hg; −0.39 ± 0.26‰, Δ^{199}Hg; −0.04 ± 0.03‰) confirm that Hg source is originated from Gumu Creek. The heterogeneous Hg distribution throughout Gumu Creek and statistically similar Hg isotope ratios between Gumu Creek and solid waste cores from the landfill suggests that the landfill collapse is the dominant source to the Hyeongsan-Gumu system. Present Hg releases is also possible given the elevated and matching Δ^{199}Hg between some riverine sediments and wastewater sampled from the landfill. The ternary mixing model estimates that the landfill collapse and wastewater releases contribute 61 ± 25 % and 22 ± 11 %, and the regional background, reflecting terrestrial runoff using deep sediment cores, explain 17 ± 24 % of Hg to

---

* Corresponding author at: Division of Environmental Science and Engineering, Pohang University of Science and Technology, 77 Cheongam-Ro, Nam-Gu, Pohang 37673, South Korea.
E-mail address: saeyunk@postech.ac.kr (S.Y. Kwon).

https://doi.org/10.1016/j.jhazmat.2023.132559
Received 12 June 2023; Received in revised form 10 August 2023; Accepted 12 September 2023
Available online 15 September 2023

the riverine sediment. We suggest that Hg isotopes can be used for routine source screening in areas where Hg sources are unknown.

1. Introduction

Mercury (Hg) is a globally distributed toxic metal, which causes neurological and reproductive impairments to wildlife and humans [1,2]. Since industrialization, anthropogenic Hg emissions have resulted in 3–5-fold Hg enrichments in global remote lake sediments [3–5]. Economic activities demanding intentional use of Hg (i.e., Hg and gold mining, manufacturing of Hg-added products, and chlor-alkali industry) have introduced substantial amount of Hg into the surrounding water and soil [6,7]. Some of the most well-known Hg contaminated sites include the Minamata Bay, Japan, and East Fork Poplar Creek, Oak Ridge, U.S., both of which are impacted by historical Hg releases leading to widespread environmental and ecological effects [8,9].

As various aspects of the environmental impacts of Hg are investigated at contaminated sites [10–12], the measurement of Hg stable isotopes has been demonstrated to be a useful tool for verifying Hg sources [13–15]. Hg reservoirs undergo mixing in the environment due to numerous physical processes, in which Hg sources with relatively distinct isotope ratios mix to varying degrees. Mass-dependent (MDF; δ^{202}Hg) and mass-independent fractionation (MIF; Δ^{199}Hg, Δ^{200}Hg) provide a multi-dimensional system in which to analyze biogeochemical processes controlling the environmental fate of Hg. Hg isotopes have been employed to verify the spatial extent of historical Hg released to the Oak Ridge area, including East Fork Poplar Creek [16] and the Clinch River [17], by quantifying percent (%) contribution of various Hg sources (i.e., coal ash spill, regional background). The MDF and MIF induced via microbial and photochemical reductions have also provided insights into horizontal and vertical transport and partitioning of Hg in East Fork Poplar Creek [18].

Thus far, the utility of Hg isotopes for source apportionment has only been verified at sites where legacy or point Hg sources have already been characterized (Table S1). The relatively distinct Hg isotope ratios in various anthropogenic and natural sources (e.g., Kwon et al. [14]) suggest its potential application for routine source screening and environmental decision-making (i.e., risk management, remediation, and liability allocation) even at newly discovered Hg contaminated sites. Here, we investigate a site within South Korea to evaluate the efficacy of Hg isotopes for source screening and decision-making at sites surrounded by multiple historical and present industrial Hg source activities. In 2016, the discovery of elevated THg levels in the sediments and soil of the Hyeongsan River and associated tributary, Gumu Creek (Pohang, South Korea), triggered a national public health issue [19,20]. The Hyeongsan River supplies regional fisheries products and supports recreational activities including sport fishing and sailing. The Hyeongsan River and Gumu Creek are surrounded by > 300 businesses and industries including the world's fifth-largest steel manufacturing facility. Moreover, in 1994, a solid waste landfill, located at the head of Gumu Creek, collapsed into the creek [20,21].

We utilize an environmental forensics (EF) approach to delineate Hg sources to the Hyeongsan River and to specifically quantify the extent of Hg influence from Gumu Creek. EF is a technique that is useful at sites with unknown sources of contamination because it draws upon a set of systematic and integrated procedures to formulate technically defensible information on the sources, responsible parties, and remedial actions [22,23]. While the application of non-traditional stable isotopes in EF has been limited relative to application of traditional stable isotopes [24,25], a number of cases have successfully employed lead (Pb), strontium (Sr), copper (Cu), zinc (Zn), and chromium (Cr) stable isotopes to build justifiable legal cases against industries that operated in contaminated riverine and groundwater systems [26–28]. In the U.S., the presence of contaminated site governance such as the Superfund Program (Comprehensive Environmental Response, Compensation, and Liability Act) has been pivotal in translating technical information into legal decisions and environmental action. The absence of such governance mechanisms in South Korea highlights the need to rely upon the guided scientific procedures to support decision-making. The aims of this study are to evaluate the efficacy of Hg stable isotopes in EF applications and to provide evidence for the importance of implementing a contaminated site governance mechanism in South Korea.

2. Materials and methods

By following the EF procedure outlined by Murphy and Morrison [29], we organize this section in the order of (1) site characterization, (2) scenario building, (3) chemical fingerprinting and/or data collection (depending on the contamination scenario), and (4) numerical analyses. Site characterization is used to generate broad understanding of the types and extents of anthropogenic activities, contaminants present in the environment, and their geographical distributions in relation to background sites. Site characterization is then used to formulate possible scenarios regarding sources, introduction pathways, and timing of release and/or emission of contaminants to the environment. The most likely scenario or proportional liability among multiple scenarios are quantified via chemical fingerprinting (Hg isotopes in this case), data collection of historical and present industrial activities, and statistical analyses.

2.1. Site characterization

The Hyeongsan River originates from Gyeongju City and flows into Yeongil Bay through Pohang City, South Korea (Fig. 1). It has a length of 62 km, watershed area of 1140 km^3, maximum width of 380 m, and a maximum depth of 5.2 m. The riverine flow rate ranges between $-$ 24 and 194 m^3/s (15 ± 21 m^3/s, n = 298) [30], with the negative flow rate suggesting the presence of back flow from Yeongil Bay to the River. Detailed hydrological and sediment dynamic assessments are currently being undertaken by the National Institute of Environmental Research (NIER). There are > 200 businesses and industries located upstream in Gyeongju City, which manufacture a diverse range of products including steel, electrical equipment, and non-ferrous metals [31]. The world's fifth-largest steel manufacturing industry is situated at the downstream of the Hyeongsan River, near Yeongil Bay, and only few kilometers away from Gumu Creek (Fig. 1). Gumu Creek, a tributary of the Hyeongsan River located 3.8 km upstream from Yeongil Bay, is an open artificial creek developed for waste drainage. The Creek spans 4.8 km in length and a maximum width of 8 m. The flow rate of the Creek ranges between 0.20 and 5.2 m^3/s near the confluence with the River. A previous investigation by Bailon et al. [19] discovered that sediments of the Hyeongsan River (0.11–36 mg/kg, n = 18) and Gumu Creek (2.8–133 mg/kg, n = 6) are severely contaminated by Hg. The types of Hg sources impacting this region and the potential Hg influence from Creek to the River have not been verified via chemical fingerprinting methods. In fact, Hyeongsan River sediments located 2.3 km upstream from the confluence with Gumu Creek also showed relatively elevated THg concentrations (1.7 mg/kg) [19], implying potential Hg transport from upstream reaches of the Hyeongsan or via adjacent terrestrial runoff and/or atmospheric deposition.

There are > 300 businesses and industries in the vicinity of Gumu Creek, which manufacture products ranging from steel, electrical equipment, chemicals, and non-ferrous metals [32] and discharge treated wastewater into the Creek. In addition, it was reported that 50,000 tons of waste in a solid waste landfill, operated by a private industry, collapsed into Gumu Creek in 1994. This waste was subsequently redeposited into the landfill as part of the incident response. In an initial survey of waste material, Jung et al. [20] found that commercial liquid Hg, phenyl-Hg, and coal ash were materials deposited in the landfill historically, with THg concentrations within the landfill reaching up to 12 mg/kg. The landfill is still in operation and any wastewater generated from the facility is discharged via an underground sewer and specifically at GSP 4.7 of the Creek (Fig. 1).

2.2. *Contamination scenarios*

Based on the site characterization, we identified four plausible and non-exclusive scenarios to describe the observation of Hg contamination in the sediments of the Hyeongsan River and Gumu Creek. The summary of the contamination scenarios and EF approach taken for each scenario is illustrated in Fig. S1. First, atmospheric emissions followed by localized deposition of Hg from the world's fifth-largest steel manufacturing industry could explain the widespread Hg contamination in the Hyeongsan River and Gumu Creek (*Scenario 1*). Second, riverine Hg transport from upstream (Gyeongju City), in the form of suspended particles, deposited to the sediments of the Hyeongsan River (*Scenario 2*). Given that the water flows from Gumu Creek into the Hyeongsan River, the upstream riverine Hg transport from Gyeongju City cannot explain Hg found within the creek. Thus, in this scenario, Gumu Creek would be impacted by Hg source other than the upstream suspended particles from the Hyeongsan River. Third, wastewater effluents and solid waste generated from multiple businesses and industries located along Gumu Creek supply Hg to the Creek and subsequently to the River via transport (*Scenario 3*). Fourth, the 1994 collapse of a solid waste landfill, situated at the head of Gumu Creek, is responsible for the widespread legacy Hg distribution in both the Creek and the River (*Scenario 4*).

2.3. *Sample and data collection*

Between April 2018 and September 2021, surface sediments along the Hyeongsan River and soil and sediments along Gumu Creek were collected (Fig. 1). Across the Hyeongsan River, sampling occurred at seven sites upstream of the confluence with Gumu Creek (HRS 0.2–HRS 6.0) and 11 sites downstream of the confluence (HRS −0.2–HRS −6.2) (Table S2). Sediment cores (1 m depth) were collected using a PVC pipe at three locations upstream of Gumu Creek confluence (HRS 0.6, 3.9, 4.4) to characterize regional background and historic Hg sources. Across Gumu Creek, 15 sediment samples at 11 locations (GCS 0.2–GCS 4.7; Table S3) and 12 soil samples at 12 locations (GCO 0.2–GCO 4.7; Table S4) were collected. Soil samples were collected from locations situated 1–8 m above the creek bed on a concrete structure built to receive treated wastewater from industrial pipes. While the concrete structure is solidified relatively uniformly across the Creek, there were substantial heterogeneity in soil type and grain size, and patches of dense vegetative cover at certain locations along the Creek. To ensure site representativeness, we collected various soil type along the entire Creek using an acid-cleaned shovel and the surface sediments (both top 5 cm) were sampled using a PVC pipe. All samples were stored in clean

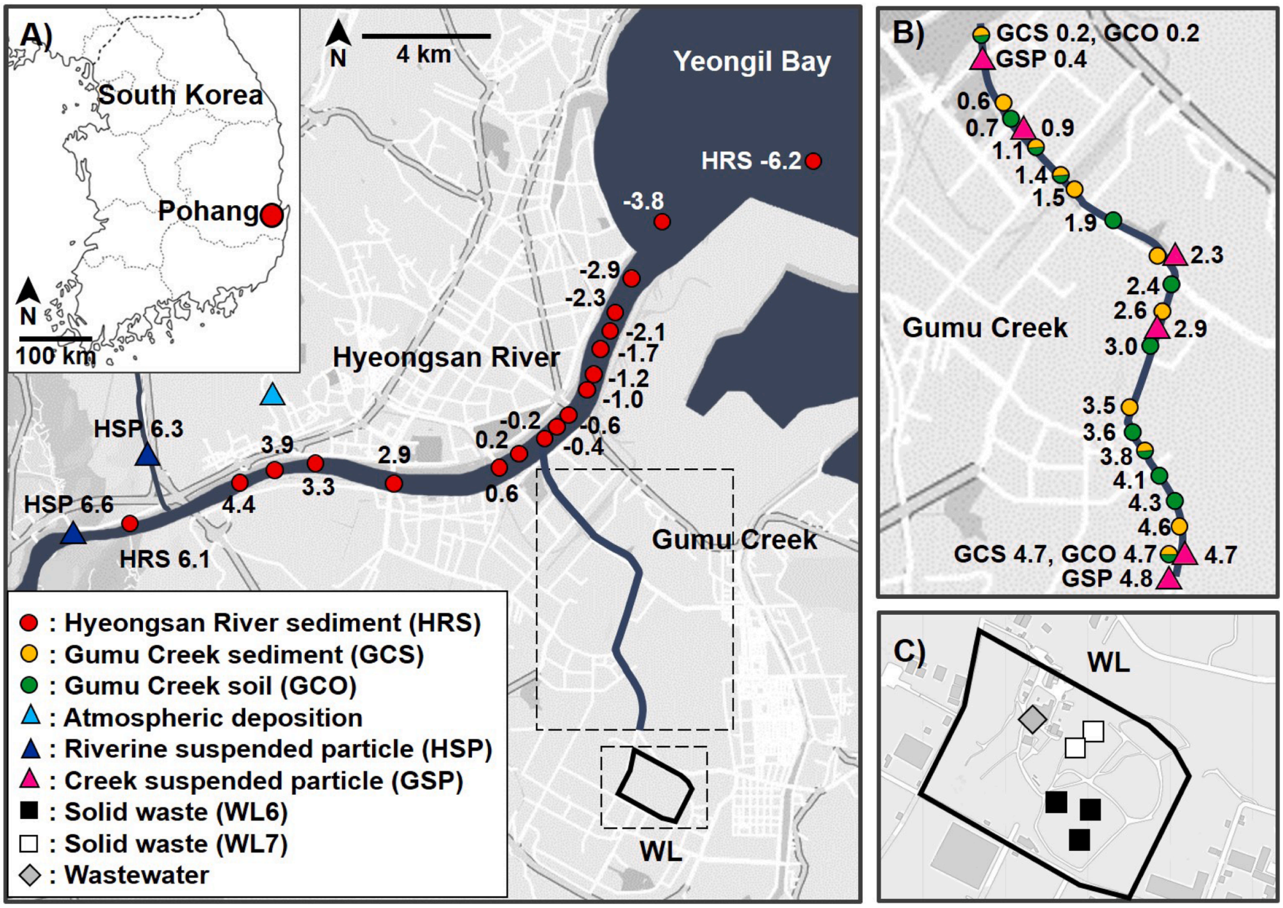

Fig. 1. Map of the A) Hyeongsan River, B) Gumu Creek, and C) waste landfill (WL) located at the city of Pohang, South Korea. The circle symbols represent the sampling sites for sediment and soil, the triangle symbols represent the sampling sites for atmospheric deposition (particulates bound mercury and precipitation) and suspended particles in water column, the square symbols represent the sampling sites for solid waste in the waste landfill and the diamond symbol represents the sampling site of wastewater in the waste landfill.

plastic bags and transported to the Environmental & Health Assessment Laboratory, Pohang University of Science and Technology, where they were lyophilized and analyzed without sieving.

To test *Scenario 1 and 2*, atmospheric particulate bound mercury (PBM), precipitation, and suspended particles of the water column (HSP) were sampled at locations across Hyeongsan River and above the confluence with Gumu Creek between January 2021 and April 2022 (Fig. 1). The PBM was collected using a high-volume air sampler (HV-1000R, Sibata) equipped with a 0.3 µm quartz filter situated on the rooftop of a building at a height of approximately 25 m. Precipitation was collected at the same site using an acid-cleaned Teflon bottle equipped with a glass p-trap and funnel, following the methods described in Motta et al. [33]. Precipitation samples (0.5–1.4 L) were treated with 1% BrCl and allowed to react for one month in dark at room temperature to ensure organic decomposition. HSP were collected during baseflow by filtering 20 L of surface water in the field through a 0.45 µm PTFE filter, and the filters were lyophilized prior to analysis.

To evaluate *Scenario 3,* we utilized a dataset gathered by the Pohang local government in 2017 and 2018 (Table S7 and S8). Upon the discovery of Hg contamination, the local government identified 50 industries which release treated wastewater into Gumu Creek, and sampled treated and untreated wastewater for Hg analyses. Solid waste samples of ash, sludge and slag were also collected and measured for THg concentration from 57 industries to verify potential illegal dumping of Hg contaminated waste. Separately, we sampled suspended particles of the water column (GSP) at six sites along Gumu Creek (GSP 0.2–4.8; Fig. 1) to investigate current Hg releases from businesses and industries including the solid waste landfill located at the head of the Creek. The GSP samples were collected on two rainy days (17 mm/day, 21 mm/day) with time periods spanning the start and end of rainfall in March and April, 2022 and by filtering 20 L of surface water through a 0.45 µm PTFE filter.

To evaluate *Scenario 4*, we collected cores of solid waste and wastewater samples from the landfill. Solid waste collected at four ranges of depths (5–6, 10–11, 15–16, 20–21 m) were sampled at two landfill sites (WL7, WL6) using a self-propelled top-hammer drill rig in April, 2020 (Fig. 1). The solid waste that collapsed into Gumu Creek and was subsequently recovered is thought to have been redeposited at the WL7 site. The semi-wet solid waste samples, extracted directly from the landfills, were frozen, freeze-dried, sieved at 150 µm, and homogenized for analyses. Five untreated and four treated wastewater were collected from the landfill between February 2021 and February 2022. The untreated wastewater includes leachate from the landfill and wastewater outsourced from nearby industries. The wastewater is then treated on site but the exact process of treatment has not been disclosed by the landfill. The general treatment processes within a solid waste landfill include outdoor suspension of large particles and/or advanced oxidation process with ultraviolet irradiation for organic chemical degradation [34,35]. After collection in 2 L bottles, samples were treated with 3 % BrCl and left for one month for organic decomposition.

2.4. Chemical analyses

THg concentrations in solid samples (sediment, soil, suspended particles, solid waste) were analyzed by atomic absorption spectroscopy (AAS; MA-3000 NIC). NIST SRM 3133 was used to generate a calibration curve and NIST SRM 2711a (Montana soil II, n = 15) was analyzed along with the samples, which showed THg recoveries between 96% and 103 % relative to the certified value (7.42 ± 0.18 mg/kg). The relative standard deviations of replicate samples were all < 10 % (n = 20). PBM collected in a quartz filter was thermally decomposed using a dual-stage furnace to release Hg, which was trapped into 8 g of 1 % $KMnO_4$ solution (in 10 % H_2SO_4). THg concentrations in liquid samples (precipitation, wastewater, PBM in 1 % $KMnO_4$ solution) were analyzed by a cold vapor atomic fluorescence spectrometry (CV-AFS; Brooks Rand). Brooks Rand $HgCl_2$ solution was used to generate a calibration curve and NIST SRM 2711a in 1 % $KMnO_4$ was analyzed between samples (n = 10), which ranged between 90 % and 98 % in THg recovery. Note that all THg concentrations are reported in dry weight (sediment, soil, suspended particles, solid waste, PBM), except for precipitation and wastewater.

Hg in both solid and liquid samples were transferred into 1 % $KMnO_4$ for Hg stable isotope analyses. Solid samples were combusted via a dual-stage furnace and preconcentrated into 8 g of 1 % $KMnO_4$. The THg recovery of the trapping procedure ranged between 89 % and 104 %. The method for Hg transfer in liquid samples is outlined by Demers et al. [36]. Briefly, 0.5 mL of 30 % $HONH_2{\cdot}HCl$ was added into 1 L of BrCl-treated samples, followed by addition of 100 mL of 10 % $SnCl_2$ for Hg^{2+} reduction. Released Hg was bubbled into 8 g of 1 % $KMnO_4$ solution. NIST RM 8610 was processed using the same method, yielding recoveries of 90–103 % (n = 3).

Hg isotopes in all $KMnO_4$ solutions were analyzed by a multi-collector inductively coupled plasma mass spectrometry (MC-ICP-MS, Nu plasma). Analysis of internal Tl standard (NIST SRM 997) and bracketing of standard–sample–standard (NIST SRM 3133) were applied to correct for instrumental mass bias. Analytical uncertainty (2 SD) of all samples was estimated based on replicate analyses of NIST SRM 2711a since it had the largest associated uncertainty. Table S5 summarizes the Hg isotope ratios of SRMs measured in this study and those reported in other laboratories. MDF, reported as δ^{202}Hg, and MIF, reported as Δ^{199}Hg, Δ^{200}Hg and Δ^{201}Hg, were calculated in units of permil (‰) referenced to NIST SRM 3133.

2.5. Numerical analysis

All numerical analyses were performed using Matlab R2022a. An independent t-test (Welch's test) was applied to determine significance of difference in Hg isotope ratios between samples (p-value <0.05). The percent (%) contributions of three Hg sources (discussed in Section 3.5) in the sediments of the Hyeongsan River were calculated using a ternary mixing model, using a combination of reciprocal of THg concentration and isotope ratio, to minimize the effect of overestimation of a Hg source contribution with a high concentration [37–40]. In the following equations below, C is defined as % Hg contribution of individual sources.

$$C_{S1} + C_{S2} + C_{S3} = 1 \tag{1}$$

$$1/THg_{sediment} = 1/THg_{S1} * C_{S1} + 1/THg_{S2} * C_{S2} + 1/THg_{S3} * C_{S3} \tag{2}$$

$$\Delta^{199}Hg_{sediment} = \Delta^{199}Hg_{S1} * C_{S1} + \Delta^{199}Hg_{S2} * C_{S2} + \Delta^{199}Hg_{S3} * C_{S3} \tag{3}$$

3. Results and discussion

3.1. Hg distribution in sediments and soils of Gumu Creek and the Hyeongsan River

Gumu Creek sediments range between 1.0 and 195 mg/kg (73 ± 61 mg/kg, 1 SD, n = 15) and Gumu Creek bank soils range between 1.4 and 75 mg/kg (35 ± 27 mg/kg, n = 12; Fig. 2A) in THg concentration. The observed THg concentrations are 2- and 4-fold higher than sediments impacted by large-scale chemical industries [10,15] and smelters [41,42]. Across the entire Gumu Creek, there are elevated THg levels with no systematic trend from upstream to downstream. This leads to our speculation that present and/or historical industrial activities have led to widespread, heterogeneous Hg distribution across the Creek. Consistent with the THg concentration, the Hg isotope ratios of the sediments and soil of Gumu Creek display no systematic changes from upstream to downstream (Fig. 3A, B). The δ^{202}Hg and Δ^{199}Hg of the sediments and soil, however, match well within a sampled site throughout the entire Creek, indicating that they are impacted by the same Hg source (Fig. 3A, B).

The Hyeongsan River sediments range in THg concentrations

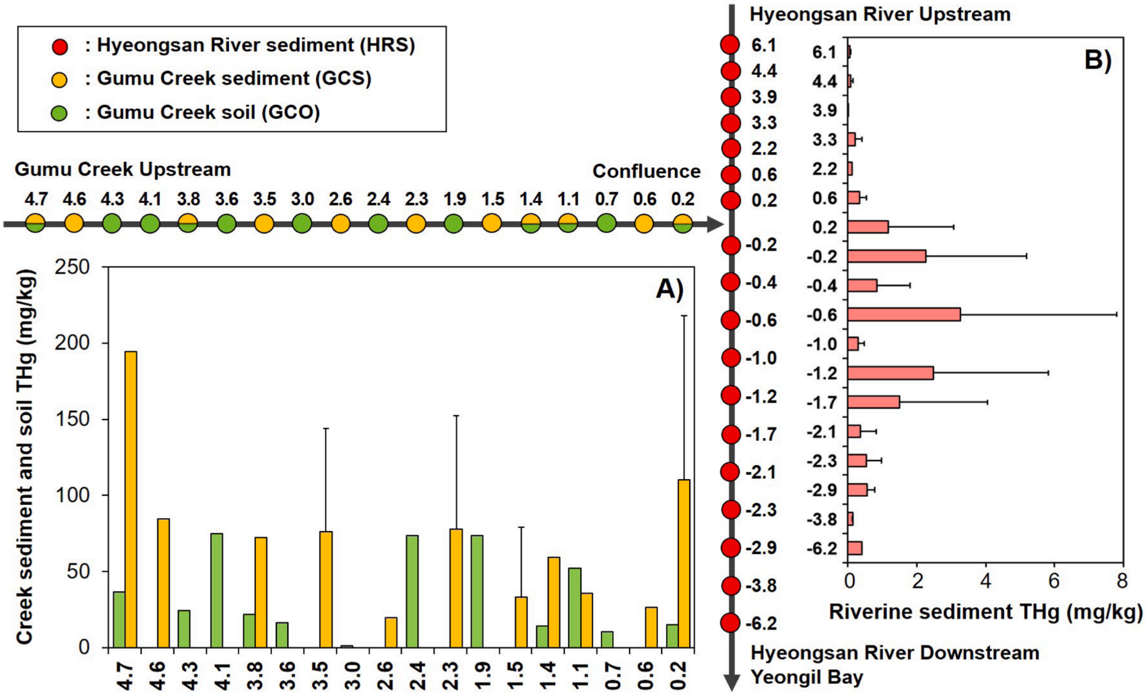

Fig. 2. Spatial distribution of THg concentration in A) the sediments of the Hyeongsan River and B) the sediments and soil of Gumu Creek. The numbers following HRS, GCS, and GCO codes indicate the distances (km) away from the confluence of the Hyeongsan River and Gumu Creek.

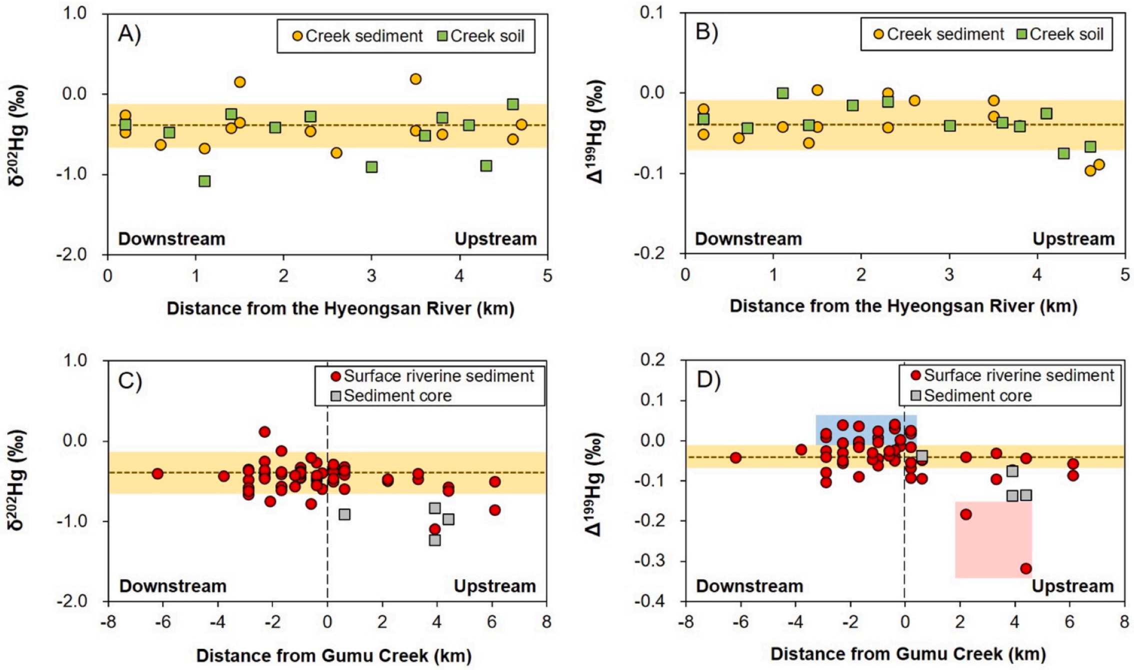

Fig. 3. A) δ^{202}Hg and B) Δ^{199}Hg of the Gumu Creek sediments and soil by distance from the Hyeongsan River and C) δ^{202}Hg and D) Δ^{199}Hg of the Hyeongsan river sediments by distance from the Creek. The horizontal dotted line and yellow shaded area represent the average and 1 SD of δ^{202}Hg and Δ^{199}Hg of Gumu Creek sediments, respectively. The red and blue shaded boxes represent two riverine sediments with low Δ^{199}Hg and several riverine sediments with high Δ^{199}Hg, respectively.

between 0.014 and 6.5 mg/kg (0.82 ± 1.5 mg/kg, n = 59) and exhibit a decreasing trend from the location where Gumu Creek joins with the River (Fig. 2B). The sediments, located upstream from the confluence with the Creek (0.48 ± 1.1 mg/kg, n = 20), display on average 2-fold lower THg concentrations than the sediments downstream of the confluence, but the values are still elevated relative to the average sediments monitored across South Korean riverine systems (0.085 ± 0.23 mg/kg, n = 352) [30]. The sediment cores collected from the River reach upstream of the confluence show low THg concentrations (0.014 ± 0.010 mg/kg, n = 60), with a decreasing concentration trend with increasing depths (Fig. S2). Based on the low THg concentrations in all sediment cores, we infer that they represent regional background conditions of Hg deposition prior to historical or present Hg contamination.

The δ^{202}Hg and Δ^{199}Hg of the Hyeongsan River sediment, including the sediment cores, exhibit small but gradual increases from upstream to downstream towards the average values of the Gumu Creek sediments (Fig. 3C, D). Some riverine sediments sampled downstream from the confluence with Gumu Creek reach Δ^{199}Hg values that are higher than the average Gumu Creek sediment, which we discuss in the section below (blue shade in Fig. 3D). Overall, the δ^{202}Hg of the Creek sediments (−0.39 ± 0.26‰, $n = 15$) are not significantly different from the δ^{202}Hg of the riverine sediments sampled both upstream and downstream from the confluence (−0.46 ± 0.17‰, $n = 59$; $p = 0.34$). The Δ^{199}Hg of the riverine (−0.04 ± 0.06‰, $n = 59$) and creek sediment (−0.04 ± 0.03‰, $n = 15$) also did not show significant Δ^{199}Hg difference ($p = 0.79$). Even the soil of Gumu Creek display no significant difference in δ^{202}Hg (−0.50 ± 0.30‰) and Δ^{199}Hg (−0.04 ± 0.02‰, $n = 12$) with the Hyeongsan riverine sediments (δ^{202}Hg; $p = 0.60$, Δ^{199}Hg; $p = 0.83$).

To briefly summarize, we observe (1) a systematic decline in the riverine sediment THg concentration with increasing distances away from the confluence with Gumu Creek, and (2) absence of significant Hg isotope difference between the Gumu Creek soil and sediment reservoirs and the downstream Hyeongsan River sediments. Based on these results, we conclude that Gumu Creek and the Hyeongsan River are impacted by a single primary Hg source, and there is substantial Hg transport from Gumu Creek to the downstream reaches of the Hyeongsan River.

To further evaluate the extent of Hg influence from Gumu Creek to the downstream Hyeongsan River, we analyze a mixing diagram for sediments of the Hyeongsan River (both surficial and deep core) against Gumu Creek sediment and soil reservoirs by plotting Hg isotope ratios in relation to THg concentration (in 1/THg) (Fig. S3). Note that the 1/THg concentrations and Hg isotope ratios of the riverine sediment samples and the residuals in regression analyses are not normally distributed (Shapiro-Wilk test, $p < 0.05$), making it difficult to assess the correlation coefficient. Nevertheless, the riverine sediments exhibit progressively increasing δ^{202}Hg toward the value of Gumu Creek from the regional background, established by the deep sediment cores in the Hyeongsan River (Fig. S3A). Only a subset of sediment cores sections were measured for Hg isotope ratios and we designate sediments sampled > 50 cm in depth as being representative of the regional background Hg for the system (Fig. S2). The regional background exhibits low THg concentrations and low δ^{202}Hg (−0.99 ± 0.18‰) and Δ^{199}Hg values (−0.10 ± 0.05‰, $n = 4$) (Fig. 3C, D), consistent with mineral soil and other terrestrial media characterized from remote forests in China and the U.S. (Fig. S4) [36,43,44]. No significant trends were observed between Δ^{199}Hg and 1/THg for the Hyeongsan-Gumu systems, which may be attributed to subtle Δ^{199}Hg variations within the riverine sediments (Fig. S3B).

Aside from the primary Hg source impacting Gumu Creek and the Hyeongsan River, we observe a subset of sediment samples with anomalous Δ^{199}Hg values. The two riverine sediments with the lowest THg concentrations (0.12 ± 0.005 mg/kg) exhibit noticeably low Δ^{199}Hg (−0.32‰ and −0.18‰), which were more negative than the deep sediment cores, reflecting the regional background. Given the low THg concentrations, it would be unlikely for an anthropogenic point Hg source to impart such negative Δ^{199}Hg. While dark abiotic reduction can result in both lower THg concentrations and lower Δ^{199}Hg in Hg^{2+} bound to sediment particles relative to sediment Hg^0, this would also shift δ^{202}Hg to a higher value within the sediments [45], which is not observed. We propose that a contribution from natural geogenic sources of Hg (i.e., mineral deposits, bedrocks), which typically have negative Δ^{199}Hg values (−0.42 to 0.10‰) [46,47], may explain this small anomalous dataset. A prior compilation of modern and pre-anthropogenic sediments from various ecosystems (river, lake, coastal, ocean) have also shown measurably lower Δ^{199}Hg in pre-anthropogenic and non-point source impacted sediments relative to point source impacted sediments, and attributed this to the contribution of natural erosion of bedrocks [14]. These two sediments, however, represent a small dataset among our sampled sediments and we thus exclude them for further source tracing. A number of riverine sediments located at downstream sites exhibit slightly higher Δ^{199}Hg (0.02 ± 0.02‰, $n = 11$) but no δ^{202}Hg differences (−0.46 ± 0.11‰, $n = 11$) when compared to the Creek sediments (Δ^{199}Hg; −0.04 ± 0.03‰, δ^{202}Hg; −0.39 ± 0.26‰) (Fig. 3D). The fact that these riverine sediments have 1.6-fold higher THg (1.3 ± 1.9 mg/kg, $n = 11$) but consistent δ^{202}Hg relative to the average riverine sediments (0.82 ± 1.5 mg/kg, $n = 59$) implies that Hg^{2+} photo-reduction, which typically induces higher δ^{202}Hg and Δ^{199}Hg in sediment-associated Hg^{2+} relative to released Hg^0 via MIF [48], is unlikely to explain the observed results. Instead, we speculate that there may be a secondary Hg source with a positive Δ^{199}Hg. Below, we combine chemical analyses, data collection, and numerical analyses to decipher the primary and secondary Hg sources.

3.2. Scenarios of anthropogenic emissions and upstream riverine transport of Hg

Based on the observed impacts of significant Hg transport from Gumu Creek to the Hyeongsan River, we rule out the influence of widespread atmospheric Hg deposition from the steel manufacturing industry (scenario 1) and upstream Hg transport from Gyeongju City (scenarios 2) as primary Hg sources. We still discuss the results of atmospheric samples and suspended particles of the water column in the Hyeongsan River to assess their roles in controlling the regional background and/or secondary Hg source isotopic compositions.

Atmospheric samples, comprising PBM (35 ± 15 pg/m^3, $n = 5$) and precipitation (26 ± 22 ng/L, $n = 8$), exhibit THg concentrations that are similar to samples collected at other Northern Hemisphere suburban locations in the U.S. and China [49,50]. The Δ^{199}Hg values of PBM (0.27 ± 0.19‰, $n = 5$; $p < 0.01$) and precipitation (0.26 ± 0.22‰, $n = 8$; $p < 0.01$) are significantly more positive than those observed in the riverine and creek sediments and soils ($n = 86$) (Fig. 4B). While some riverine sediments located at the downstream from the confluence with Gumu Creek have slightly higher Δ^{199}Hg (blue shade in Fig. 3D), it would be unlikely for atmospheric Hg deposition at the current magnitude to overprint Δ^{199}Hg of the riverine sediments and at only specific regions within the River.

As for the upstream influence, the THg concentrations in the suspended particles of the Hyeongsan River (HSP) exhibit levels (0.32 ± 0.32 mg/kg, $n = 4$) that are similar to remote riverine systems reported previously [51,52]. The δ^{202}Hg of the HSP are distinctly more negative (−1.73 ± 0.70‰, $n = 4$) than the surface sediments of the Hyeongsan River (Fig. 4B). The highly negative δ^{202}Hg of the HSP are consistent with the compiled terrestrial media [36,43,44], which has wide δ^{202}Hg ranges, and overlap with the regional background (deep sediment cores) (Fig. S4). This implies that the HSP is sourced from the adjacent terrestrial runoff rather than from upstream industries at Gyeongju City and supplies regional background Hg to the Hyeongsan River.

3.3. Scenarios of Hg transport from Gumu Creek

Exploring the hypothesis that the primary Hg source of the Hyeongsan River originates from Gumu Creek, we examine the local governmental data reporting THg concentrations in wastewater and solid waste from ~57 industries, which discharge treated wastewater to the Creek (scenario 3) (Table S7, Table S8). The treated (0–0.001 mg/L) and untreated wastewater (0–0.028 mg/L) and solid waste (0–0.15 mg/kg) show overall low THg concentrations, indicating that industrial Hg releases and potential illegal dumping of solid waste cannot explain the observed THg concentrations across the Creek. In addition, the list of chemicals and products purchased, imported, and manufactured by these industries did not show any evidence of intentional Hg use (i.e.,

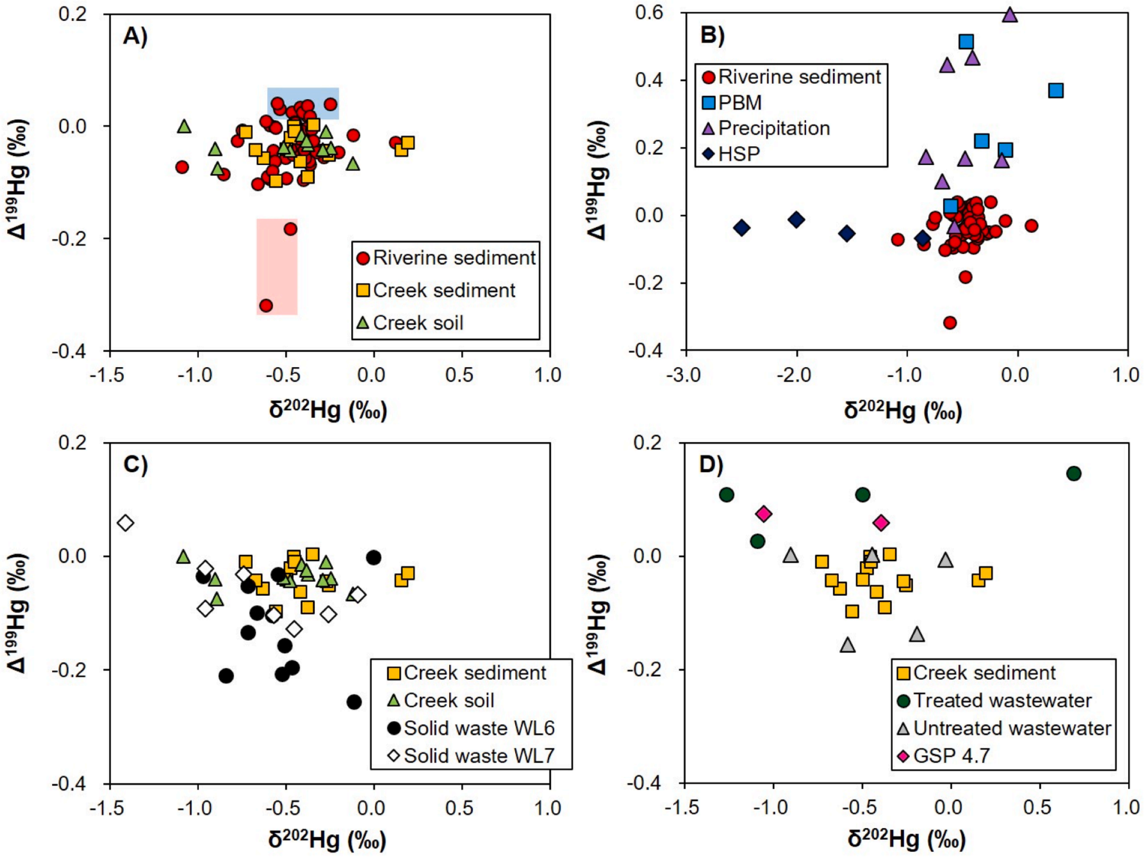

Fig. 4. δ^{202}Hg and Δ^{199}Hg of A) the Hyeongsan River and the Gumu Creek sediments and soil, B) the riverine sediments, atmospheric particulate bound mercury (PBM), precipitation, and suspended particles in the Hyeongsan River (HSP), C) the Creek sediments and soil, and solid wastes from the solid waste landfills (WL6, WL7), D) the Creek sediments, wastewater from the landfill, and suspended particles of the water column at GSP 4.7 of the Gumu Creek. The red and blue shaded boxes represent two riverine sediments with low Δ^{199}Hg and several riverine sediments with high Δ^{199}Hg, respectively.

Hg-added products, catalysts).

The influence of solid waste landfill is explored by evaluating Hg concentrations and isotope ratios in the solid waste cores (historical collapse; scenario 4) and wastewater (present releases; scenario 3) collected from the landfill. Note that this is the first study to characterize Hg isotope ratios in a variety of waste materials generated from a landfill. The THg concentrations of the solid waste cores are similar to that of creek sediments and soil, with WL7 (35 ± 81 mg/kg, maximum; 234 mg/kg, $n = 8$) displaying higher THg concentrations than WL6 (4.6 ± 7.7 mg/kg, maximum; 23 mg/kg, $n = 12$). The untreated wastewater samples exhibit, on average, 850-fold higher THg concentrations (1797 ± 3988 μg/L, maximum; 8932 μg/L, $n = 5$) relative to the treated wastewater (2.1 ± 2.5 μg/L, maximum; 4.7 μg/L, $n = 4$), which is subject to regular discharge from the landfill (see Section 2.1). As for the Hg isotopes, the solid waste cores from WL7 and WL6 exhibit similar δ^{202}Hg ranges (WL7; −0.68 ± 0.43‰, WL6; −0.55 ± 0.27‰) but significantly more positive Δ^{199}Hg in WL7 (−0.06 ± 0.06‰) than WL6 (−0.12 ± 0.08‰) ($p = 0.03$) (Fig. 4C). Similarly, the untreated and treated wastewater share comparable δ^{202}Hg ranges but the treated samples have higher Δ^{199}Hg relative to the untreated samples (Fig. 4D). The Δ^{199}Hg difference between the WL6 and WL7 is likely caused by different types or proportions of waste deposited into the landfills. In a recent Hg isotope characterization of the waste deposited into the WL6 (same landfill), Jung et al. [20] reported that coal ash has more negative Δ^{199}Hg (−0.30‰) relative to phenyl-Hg, used as biocide, and commercial liquid Hg, incorporated in Hg-added products (both near-zero Δ^{199}Hg). The absence of depth-related pattern in THg concentrations within the waste cores (Fig. S5) implies that heterogenous distribution of various solid waste explain the Δ^{199}Hg difference between the WL6 and WL7. In regards to the wastewater, the elevated Δ^{199}Hg in the treated wastewater is intriguing and we think that the dissolved Hg fractions within the treated wastewater are subjected to a higher extent of Hg^{2+} photo-reduction relative to the untreated wastewater. As mentioned, the general treatment processes within a landfill include outdoor suspension of solid materials and/or ultraviolet irradiation for organic chemical degradation [34,35]. Both processes would result in much lower particulate bound Hg fractions in treated wastewater than untreated wastewater, which is what we observed (93 % vs. 42 % particulate bound Hg in the untreated and treated wastewater, respectively) (Table S9). The remaining Hg within the dissolved phases are likely subjected to Hg^{2+} photo-reduction from an outdoor setting or via ultraviolet irradiation, resulting in an elevated Δ^{199}Hg in Hg^{2+} relative to the released Hg^0. Further studies would be needed to understand how treatment processes modify Hg isotope ratios in the waste materials, as they may have substantial downstream influences.

More importantly, the statistical tests confirm that the δ^{202}Hg and Δ^{199}Hg of the Gumu Creek soils and sediment ($n = 27$) are not significantly different from the WL7 waste cores (δ^{202}Hg; $p = 0.16$, Δ^{199}Hg; $p = 0.32$), where the collapsed waste from the 1994 incident was redeposited. Gumu Creek soils and sediment ($n = 27$) do not display a significant difference from the untreated landfill wastewater (δ^{202}Hg; $p = 0.69$, Δ^{199}Hg; $p = 0.89$). Statistically significant δ^{202}Hg and Δ^{199}Hg differences are observed between the Gumu Creek sediment and soil ($n = 27$) and the WL6 waste cores ($n = 12$) and treated wastewater ($n = 5$). Based on these results, we conclude that the historical collapse of the solid waste landfill is the primary Hg source to Gumu Creek (scenario 4). The observation of elevated THg concentrations and consistent Hg isotope ratios between the sediment and soil of Gumu

Creek implies that a large-scale collapse of landfill can only explain the widespread Hg contamination across the Creek. A prior study has reported that most of Hg found in the creek sediments are strongly bound with sulfur, by forming Hg-sulfide [53]. This indicates that there is slow Hg mobilization and absence of significant Hg isotope fractionation within the creek bed, leading to long-term preservation of the source Hg isotope signatures derived from the historical waste landfill collapse. The Hg sources from Gumu Creek are then exported to the Hyeongsan River via sediment transport, which is confirmed by the statistically similar Hg isotope ratios between the surface sediments of Gumu Creek and the Hyeongsan River and different isotope ratios between the surface and deep riverine sediments.

3.4. *Secondary Hg source*

Aside from the primary Hg source, the positive Δ^{199}Hg observed in several riverine sediments, but not in soil, suggest that there may be a secondary Hg source in the form of releases. Environmentally-induced MIF in sediments is unlikely to explain the positive Δ^{199}Hg values of sediments given the elevated THg concentrations relative to the average riverine sediments. Additionally, processes that induce significant MIF (e.g. photochemical reduction) would also result in large δ^{202}Hg shifts, which are not observed. Positive Δ^{199}Hg values are observed in all of the analyzed treated wastewater from the solid waste landfill (Fig. 4D), which leads to our hypothesis that regular discharge of treated wastewater, which contains Hg that is relatively more mobile and conducive to rapid transport, may be impacting the sediments.

To verify the influence of treated wastewater discharge on the Hg reservoirs within Gumu Creek and Hyeongsan River, we compare THg concentrations and Hg isotope ratios between the treated wastewater and the suspended particles in the water column of Gumu Creek (GSP). Note that the GSP were sampled prior to and after two rain events to verify the isotopic composition of this source when conditions are conducive to rapid release and transport across Gumu Creek and to the Hyeongsan River. As illustrated in Fig. 5, the THg concentrations in the GSP are relatively uniform prior to rain events and likely reflect Hg resuspended from the sediments given the comparably elevated THg concentrations (614 ± 389 mg/kg, n = 12) with those of the creek sediments. A few hours after each rain event, the flow rate of the Creek increased from 0.65 to 5.2 m^3/s (first rain) and 0.38–1.5 m^3/s (second rain), respectively, and large THg peaks are observed, particularly at GSP 4.7, where treated wastewater from the solid waste landfill is discharged through an underground sewer to the Creek. GSP 4.8 displayed the lowest THg concentrations, even during the rain events, and is located upstream from GSP 4.7 adjacent to where discharge from an urban stormwater pipe enters the Creek. The distinct THg peak observed at GSP 4.7 indicates that wastewater drained from the solid waste landfill has a widespread downstream Hg effect to Gumu Creek. The THg concentration peaks are associated with peaks in Δ^{199}Hg, particularly during the second rain event (Fig. 5B), and display Δ^{199}Hg values that are much higher than the average Gumu Creek sediment but more similar to the treated wastewater. Based on these results, we presume that the mixtures of Hg discharged from the wastewater, with a positive Δ^{199}Hg, and Hg resuspended from the creek sediment, which has a high THg concentration, are transported and deposited to the downstream Hyeongsan River sediments during rain events. The low THg concentrations measured in the treated wastewater is puzzling and we speculate, without further direct evidence, that there may be intermittent releases of high Hg wastewater during rain/storm events. Such high concentration wastewater releases would lead to an overflow of water load capacity within the treatment plant, resulting in the release of a Hg source that could have an isotopic influence in the Hyeongsan River sediments. We emphasize that our speculation relies upon the elevated and matching Δ^{199}Hg between a limited number of samples of the treated wastewater, suspended particles during rain events, and some sediments from the Hyeongsan River. Regular sampling of the treated wastewater and suspended particles in the water column of Gumu Creek and exact mechanisms leading to the positive Δ^{199}Hg in the treated wastewater would be crucial for verifying our hypothesis.

3.5. *Hg source attribution*

The primary (historical collapse; scenario 4) and secondary Hg sources (treated wastewater release; scenario 3), and the regional background are designated as end-members to quantify the percent (%) contribution to the Hyeongsan River sediments. In our ternary mixing model (described in detail in Section 2.5), we apply the average THg concentration and average Δ^{199}Hg of the WL7 waste core (35 mg/kg, Δ^{199}Hg; −0.06‰, n = 8), the treated wastewater (98 mg/kg, Δ^{199}Hg; 0.10‰, n = 4), and the sediment cores sampled at > 50 cm depth

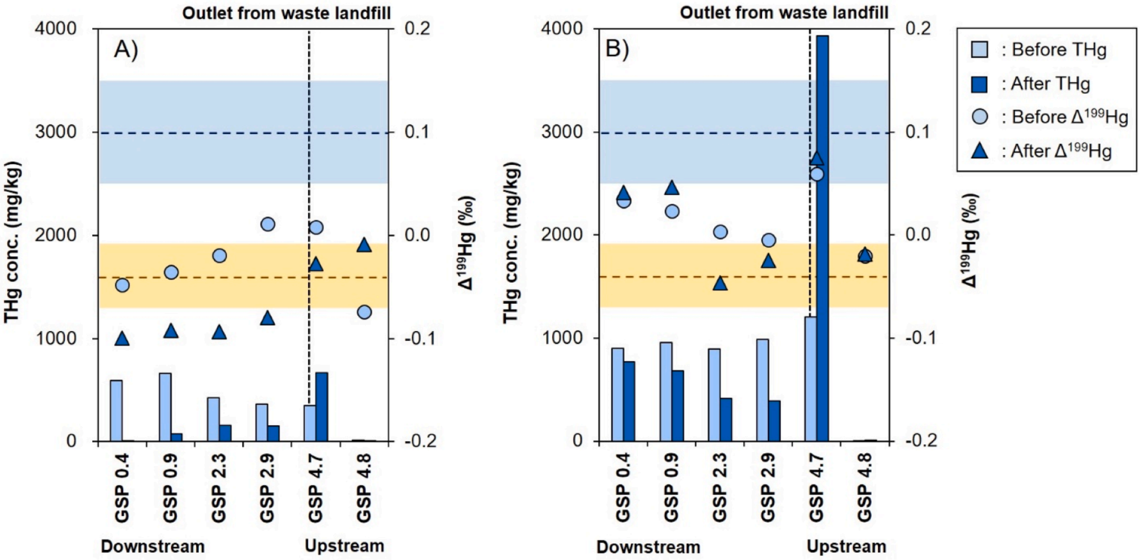

Fig. 5. THg concentration and Δ^{199}Hg of the suspended particles of the water column in Gumu Creek (GSP) A) in the first and B) second rain events. Blue dotted line and shaded area represent the average Δ^{199}Hg of the treated wastewater (n = 4) and 1 SD, respectively. Yellow dotted line and shaded area represent the average Δ^{199}Hg of the creek sediments (n = 15) and 1 SD, respectively.

(0.013 mg/kg, Δ^{199}Hg; −0.10‰, n = 4) to represent end-members. Treated wastewater, suspended particles in Gumu Creek, and some of the riverine sediments exhibited significantly high Δ^{199}Hg values, which together can serve as a single Hg source end-member, although a clear hypothesis for high Δ^{199}Hg in the treated wastewater is still lacking. The similar average δ^{202}Hg values in the WL7 waste core and treated wastewater makes it difficult to include δ^{202}Hg in the mixing model. Nevertheless, we note that the δ^{202}Hg ranges of both wastes encompass the δ^{202}Hg ranges of the riverine and creek sediments and the similar averages can be explained by the degree of heterogeneity in the waste samples (Fig. S7). In the earlier binary mixing model of using the Gumu creek sediments and the regional background as end-members, we observe no significant relationship between Δ^{199}Hg and 1/THg (Fig. S3B). When taking account of the treated wastewater with a positive Δ^{199}Hg, most sediments of the Hyeongsan River are well distributed among the three end-member Hg sources (Fig. 6A). Several sediment samples exhibited characteristics that were not representable as mixtures of the chosen end-members, resulting in negative % contribution from a source. In this case, negative % contributions were set to zero and % contributions from other Hg sources were proportionally re-calculated.

As illustrated in Fig. 6B, the estimated % Hg contribution in Hyeongsan River sediments of the primary Hg source, secondary Hg source, and the regional background source are 61 ± 25 %, 22 ± 11 %, and 17 ± 24 %, respectively. Uncertainty of % Hg contribution, calculated by adding and subtracting analytical uncertainly (2 SD) of 0.03‰ from a sample value, is as high as ± 19% for the solid waste cores and the treated wastewater, and up to ± 13 % for the regional background (sediment cores). Even after considering the uncertainty, the % Hg contribution from the regional background, supplied by terrestrial runoff, and the primary Hg source are the highest in the upstream. The high proportional contribution of the primary Hg source in the upstream sediments is likely owed to the fact that the solid waste transported from Gumu Creek to the Hyeongsan River has been subjected to upstream migration via intermittent ebb flow from Yeongil Bay since the event of collapse in 1994. This may also explain the consistently elevated % contribution of the primary Hg source (7–84 %) in the downstream of the Hyeongsan River. Most Hg introduced via the historical landfill collapse was likely associated with the particles of solid waste, making landfill-released Hg more conducive to deposition to the creek and riverine sediment bed and less prone to relatively fast transport downstream. Conversely, the secondary Hg source, which is conducive to transport through the Creek and riverine water current during rain/storm events, are mostly observed in the downstream of the Hyeongsan River. We find that the simultaneous actions of remedial measures on the legacy Hg that originated from the landfill collapse, in combination with stringent regulations on the current release of Hg within wastewater would benefit the remediation of the Hyeongsan River sediments.

4. Conclusion

The effectiveness of using Hg isotopes for source apportionment has only been confirmed in areas where legacy or point Hg sources have already been thoroughly researched (Table S1). Our study serves as a powerful example that Hg isotopes can be used for routine source screening and decision-making even in areas with unknown sources. Here, we estimate that the solid waste collapsed in 1994 and on-going releases of treated wastewater are responsible for 61 ± 25 % and 22 ± 11 % of accumulated Hg, respectively, in the Hyeongsan River sediments. On the contrary, the large-scale atmospheric Hg emissions from the steel manufacturing industries and the riverine Hg transport from upstream have little impact on the riverine sediments. Taking the EF approach was particularly effective in building plausible contamination scenarios, which is important not only for delineating the source of contamination but also ruling out irrelevant sources. The large steel manufacturing industry and adjacent industrial complex were initially speculated as the major Hg contributors by the public, given the long duration and active operations of these industries. Industrial activities taking place at the upstream of the Hyeongsan River, in the city of Gyeongju, also cannot be disregarded. We suggest that future investigation is needed to understand precisely the contribution of widespread and regional atmospheric Hg deposition to the Hyeongsan-Gumu system.

We expect that the utility of Hg isotopes will grow further with the expansion of international governance on Hg. The UNEP's Minamata Convention on Mercury, initiated in 2017, has specific provisions on contaminated sites (Article 12), which requires individual nations to develop regulatory and scientific tools to screen Hg sources and prioritize contaminated sites [54]. Although the South Korean government, which is a party to the Convention, has been working to follow these guidelines, there is currently no governing program within South Korea for sites that have been identified as Hg-contaminated. This study serves as a useful framework for investigation of sites, with known or suspected Hg-impacts, in South Korea or around the world.

Environmental Implication

The Minamata Convention on Mercury emphasizes the need to

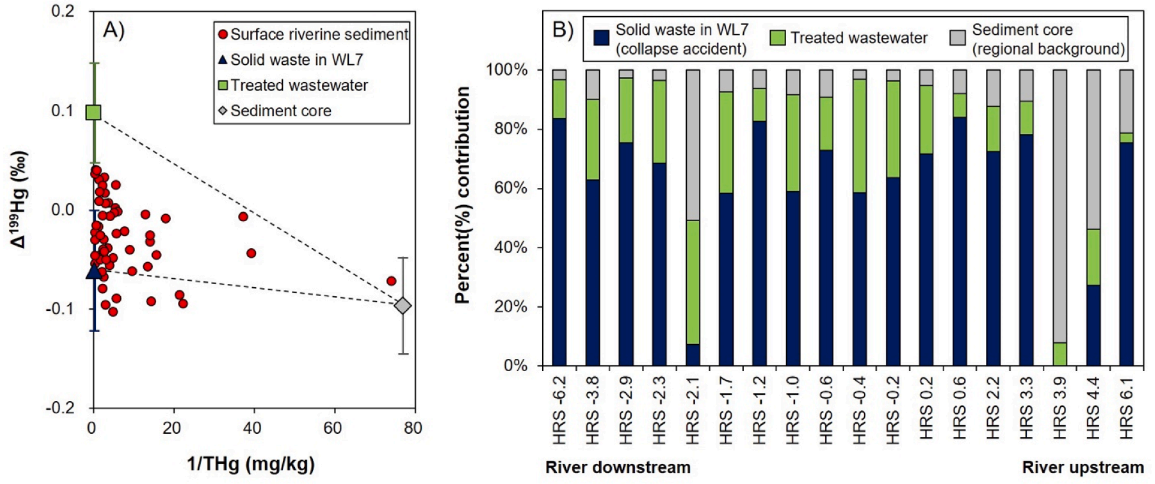

Fig. 6. A) Δ199Hg and 1/THg of the Hyegonsan River surface sediments and the three Hg source end-members of the WL7 waste core, treated wastewater, and the sediment core (regional background). B) Estimated percent (%) Hg contribution of the three sources to the Hyeongsan River sediments.

develop scientific framework for source screening and management of mercury contaminated sites. We use an environmental forensics approach as a scientific framework and mercury stable isotopes as a source screening tool to delineate mercury sources in a contaminated river within South Korea. Mercury isotopes for source apportionment has been limited to sites where point mercury sources have been well characterized. In contrary to the prior studies, our study evaluates the efficacy of mercury isotopes at site where sources are unknown and illustrates the importance of drawing upon the environmental forensics application.

CRediT authorship contribution statement

Sae Yun Kwon: Supervision, Conceptualization, Methodology. **Young Gwang Kim:** Conceptualization, Methodology, Formal analysis, Investigation, Writing - Original Draft. **Spencer J. Washburn:** Writing - Review & Editing. **Yongseok Hong:** Investigation, Writing - Review & Editing. **Seung Hee Han:** Investigation, Writing - Review & Editing. **Mikyung Lee:** Validation, Writing - Review & Editing. **Ji Hyoung Park:** Validation, Writing - Review & Editing.

Declaration of Competing Interest

The authors declare that they have no known competing financial interests or personal relationships that could have appeared to influence the work reported in this paper.

Data availability

Data will be made available on request.

Acknowledgments

No conflict of interest to declare. This work was supported by the National Research Foundation of Korea (NRF) funded by the Korean Government (MSIT) [NRF-2021R1C1C1008429]; the National Institute of Environmental Research (NIER) funded by the Korean Government (ME) [NIER-2020–04-02–073]; and the Korea Institute of Marine Science & Technology Promotion (KIMST) funded by the Korean Government (MOF) [KIMST-20220534].

Appendix A. Supporting information

Supplementary data associated with this article can be found in the online version at doi:10.1016/j.jhazmat.2023.132559.

References

[1] Barst, B.D., Chételat, J., Basu, N., 2022. Toxicological risk of mercury for fish and invertebrate prey in the Arctic. Sci Total Environ 836, 155702. https://doi.org/10.1016/j.scitotenv.2022.155702.

[2] Mergler, D., Anderson, H.A., Chan, L.H.M., Mahaffey, K.R., Murray, M., Sakamoto, M., et al., 2007. Methylmercury exposure and health effects in humans: a worldwide concern. Ambio 36 (1), 3–11. https://doi.org/10.1579/0044-7447(2007)36[3:MEAHEI]2.0.CO;2.

[3] Amos, H.M., Sonke, J.E., Obrist, D., Robins, N., Hagan, N., Horowitz, H.M., et al., 2015. Observational and modeling constraints on global anthropogenic enrichment of mercury. Environ Sci Technol 49 (7), 4036–4047. https://doi.org/10.1021/es5058665.

[4] Lee, J.H., Kwon, S.Y., Yin, R., Motta, L.C., Kurz, A.Y., Nam, S.I., 2021. Spatiotemporal characterization of mercury isotope baselines and anthropogenic influences in lake sediment cores. Glob Biogeochem Cycle 35 (10), e2020GB006904. https://doi.org/10.1029/2020GB006904.

[5] Lepak, R.F., Janssen, S.E., Engstrom, D.R., Krabbenhoft, D.P., Tate, M.T., Yin, R., et al., 2020. Resolving atmospheric mercury loading and source trends from isotopic records of remote North American lake sediments. Environ Sci Technol 54 (15), 9325–9333. https://doi.org/10.1021/acs.est.0c00579.

[6] Horowitz, H.M., Jacob, D.J., Amos, H.M., Streets, D.G., Sunderland, E.M., 2014. Historical mercury releases from commercial products: global environmental implications. Environ Sci Technol 48 (17), 10242–10250. https://doi.org/10.1021/es501337j.

[7] Streets, D.G., Horowitz, H.M., Jacob, D.J., Lu, Z., Levin, L., Ter Schure, A.F., et al., 2017. Total mercury released to the environment by human activities. Environ Sci Technol 51 (11), 5969–5977. https://doi.org/10.1021/acs.est.7b00451.

[8] Yokoyama, H., 2018. Mercury Pollution in Minamata. Springer Nature. https://doi.org/10.1007/978-981-10-7392-2.

[9] Brooks, S.C., Southworth, G.R., 2011. History of mercury use and environmental contamination at the Oak ridge Y-12 plant. Environ Pollut 159 (1), 219–228. https://doi.org/10.1016/j.envpol.2010.09.009.

[10] Feng, X., Foucher, D., Hintelmann, H., Yan, H., He, T., Qiu, G., 2010. Tracing mercury contamination sources in sediments using mercury isotope compositions. Environ Sci Technol 44 (9), 3363–3368. https://doi.org/10.1021/es9039488.

[11] Kocman, D., Horvat, M., Pirrone, N., Cinnirella, S., 2013. Contribution of contaminated sites to the global mercury budget. Environ Res 125, 160–170. https://doi.org/10.1016/j.envres.2012.12.011.

[12] Wang, J., Feng, X., Anderson, C.W., Xing, Y., Shang, L., 2012. Remediation of mercury contaminated sites – a review. J Hazard Mater 221, 1–18. https://doi.org/10.1016/j.jhazmat.2012.04.035.

[13] Blum, J.D., Sherman, L.S., Johnson, M.W., 2014. Mercury isotopes in earth and environmental sciences. Annu Rev Earth Planet Sci 42, 249–269. https://doi.org/10.1146/annurev-earth-050212-124107.

[14] Kwon, S.Y., Blum, J.D., Yin, R., Tsui, M.T.-K., Yang, Y.H., Choi, J.W., 2020. Mercury stable isotopes for monitoring the effectiveness of the Minamata convention on mercury. Earth Sci Rev 203, 103111. https://doi.org/10.1016/j.earscirev.2020.103111.

[15] Wiederhold, J.G., Skyllberg, U., Drott, A., Jiskra, M., Jonsson, S., Bjorn, E., et al., 2015. Mercury isotope signatures in contaminated sediments as a tracer for local industrial pollution sources. Environ Sci Technol 49 (1), 177–185. https://doi.org/10.1021/es5044358.

[16] Donovan, P.M., Blum, J.D., Demers, J.D., Gu, B., Brooks, S.C., Peryam, J., 2014. Identification of multiple mercury sources to stream sediments near Oak Ridge, TN, USA. Environ Sci Technol 48 (7), 3666–3674. https://doi.org/10.1021/es4046549.

[17] Bartov, G., Deonarine, A., Johnson, T.M., Ruhl, L., Vengosh, A., Hsu-Kim, H., 2013. Environmental impacts of the Tennessee Valley Authority Kingston coal ash spill. 1. Source apportionment using mercury stable isotopes. Environ Sci Technol 47 (4), 2092–2099. https://doi.org/10.1021/es303111p.

[18] Demers, J.D., Blum, J.D., Brooks, S.C., Donovan, P.M., Riscassi, A.L., Miller, C.L., et al., 2018. Hg isotopes reveal in-stream processing and legacy inputs in East Fork Poplar Creek, Oak Ridge, Tennessee, USA. Environ Sci Process Impacts 20 (4), 686–707. https://doi.org/10.1039/c7em00538e.

[19] Bailon, M.X., David, A.S., Park, Y., Kim, E., Hong, Y., 2018. Total mercury, methyl mercury, and heavy metal concentrations in Hyeongsan River and its tributaries in Pohang city, South Korea. Environ Monit Assess 190 (5), 1–16. https://doi.org/10.1007/s10661-018-6624-4.

[20] Jung, S., Kwon, S.Y., Hong, Y., Yin, R., Motta, L.C., 2021. Isotope investigation of mercury sources in a creek impacted by multiple anthropogenic activities. Chemosphere 282, 130947. https://doi.org/10.1016/j.chemosphere.2021.130947.

[21] Munhwa Broadcasting Corporation, 1994. Collapse of a landfill in the Pohang Steel Industrial Complex. <〈https://imnews.imbc.com/replay/1994/nwdesk/article/1931605_30690.html〉>. (Accessed May 22 2023).

[22] Philp, R.P., 2015. Application of Stable Isotopes and Radioisotopes in Environmental Forensics. Elsevier. https://doi.org/10.1016/B978-0-12-404696-2.00011-4.

[23] Stout, S.A., Uhler, A.D., Naymik, T.G., McCarthy, K.J., 1998. Peer reviewed: environmental forensics unraveling site liability. Environ Sci Technol 32 (11), 260A–264A.

[24] Cerling, T.E., Barnette, J.E., Bowen, G.J., Chesson, L.A., Ehleringer, J.R., Remien, C.H., et al., 2016. Forensic stable isotope biogeochemistry. Annu Rev Earth Planet Sci 44, 175–206. https://doi.org/10.1146/annurev-earth-060115-012303.

[25] Philp, R.P., 2007. The emergence of stable isotopes in environmental and forensic geochemistry studies: a review. Environ Chem Lett 5, 57–66. https://doi.org/10.1007/s10311-006-0081-y.

[26] Aggarwal, J., Habicht-Mauche, J., Juarez, C., 2008. Application of heavy stable isotopes in forensic isotope geochemistry: a review. Appl Geochem 23 (9), 2658–2666. https://doi.org/10.1016/j.apgeochem.2008.05.016.

[27] Miller, J.R., 2013. Forensic assessment of metal contaminated rivers in the 21st century using geochemical and isotopic tracers. Minerals 3 (2), 192–246. https://doi.org/10.3390/min3020192.

[28] Pontér, S., Sutliff-Johansson, S., Engström, E., Widerlund, A., Mäki, A., Rodushkina, K., et al., 2020. Evaluation of a multi-isotope approach as a complement to concentration data within environmental forensics. Minerals 11 (1), 37. https://doi.org/10.3390/min11010037.

[29] Murphy, B.L., Morrison, R.D., 2014. Introduction to Environmental forensics. Elsevier,. https://doi.org/10.1016/C2012-0-01202-1.

[30] National Institute of Environmental Research, 2021. Water environment information system. <〈https://water.nier.go.kr/web〉>. (Accessed May 22 2023).

[31] Gyeongju government, 2023. Occupancy status of industrial complex in Gyeongju. <〈https://url.kr/75nwui〉>. (Accessed May 22 2023).

[32] Pohang iron and steel industrial complex administration corporation 2023. Occupancy status. <〈http://www.phsic.or.kr/www/area/classify.html〉>. (Accessed May 22 2023).

[33] Motta, L.C., Blum, J.D., Johnson, M.W., Umhau, B.P., Popp, B.N., Washburn, S.J., et al., 2019. Mercury cycling in the North Pacific subtropical gyre as revealed by mercury stable isotope ratios. Glob Biogeochem Cycle 33 (6), 777–794. https://doi.org/10.1029/2018GB006057.

[34] Crini, G., Lichtfouse, E., 2019. Advantages and disadvantages of techniques used for wastewater treatment. Environ Chem Lett 17, 145–155. https://doi.org/10.1007/s10311-018-0785-9.

[35] Miklos, D.B., Remy, C., Jekel, M., Linden, K.G., Drewes, J.E., Hübner, U., 2018. Evaluation of advanced oxidation processes for water and wastewater treatment – a critical review. Water Res 139, 118–131. https://doi.org/10.1016/j.watres.2018.03.042.

[36] Demers, J.D., Blum, J.D., Zak, D.R., 2013. Mercury isotopes in a forested ecosystem: Implications for air-surface exchange dynamics and the global mercury cycle. Glob Biogeochem Cycle 27 (1), 222–238. https://doi.org/10.1002/gbc.20021.

[37] Donovan, P.M., Blum, J.D., Yee, D., Gehrke, G.E., Singer, M.B., 2013. An isotopic record of mercury in San Francisco Bay sediment. Chem Geol 349, 87–98. https://doi.org/10.1016/j.chemgeo.2013.04.017.

[38] Zhang, R., Russell, J., Xiao, X., Zhang, F., Li, T., Liu, Z., et al., 2018. Historical records, distributions and sources of mercury and zinc in sediments of East China sea: implication from stable isotopic compositions. Chemosphere 205, 698–708. https://doi.org/10.1016/j.chemosphere.2018.04.100.

[39] Liu, J., Wang, L., Wang, J., Zhang, Q., Wei, X., Lin, Y., et al., 2022. Quantification of smelter-derived contributions to thallium contamination in river sediments: novel insights from thallium isotope evidence. J Hazard Mater 424, 127594. https://doi.org/10.1016/j.jhazmat.2021.127594.

[40] Liu, J., Yuan, W., Wei, X., Liu, Y., Huang, Y., Wang, J., 2023. Stable thallium (Tl) isotopic signature as a reliable source tracer in river sediments impacted by mining activities. J Hazard Mater 448, 130859. https://doi.org/10.1016/j.jhazmat.2023.130859.

[41] Sonke, J.E., Schäfer, J., Chmeleff, J., Audry, S., Blanc, G., Dupré, B., 2010. Sedimentary mercury stable isotope records of atmospheric and riverine pollution from two major European heavy metal refineries. Chem Geol 279 (3–4), 90–100. https://doi.org/10.1016/j.chemgeo.2010.09.017.

[42] Sun, R., Hintelmann, H., Wiklund, J.A., Evans, M.S., Muir, D., Kirk, J.L., 2022. Mercury isotope variations in lake sediment cores in response to direct mercury emissions from non-ferrous metal smelters and legacy mercury remobilization. Environ Sci Technol. https://doi.org/10.1021/acs.est.2c02692.

[43] Wang, X., Luo, J., Yin, R., Yuan, W., Lin, C.-J., Sommar, J., et al., 2017. Using mercury isotopes to understand mercury accumulation in the montane forest floor of the Eastern Tibetan Plateau. Environ Sci Technol 51 (2), 801–809. https://doi.org/10.1021/acs.est.6b03806.

[44] Zheng, W., Obrist, D., Weis, D., Bergquist, B.A., 2016. Mercury isotope compositions across North American forests. Glob Biogeochem Cycle 30 (10), 1475–1492. https://doi.org/10.1002/2015GB005323.

[45] Zheng, W., Hintelmann, H., 2010. Nuclear field shift effect in isotope fractionation of mercury during abiotic reduction in the absence of light. J Phys Chem A 114 (12), 4238–4245. https://doi.org/10.1021/jp910353y.

[46] Deng, C., Zhang, J., Hu, R., Luo, K., Zhu, Y., Yin, R., 2022. Mercury isotope constraints on the genesis of late Mesozoic Sb deposits in South China. Sci China-Earth Sci 1–13. https://doi.org/10.1007/s11430-021-9851-x.

[47] Liu, Y.-F., Qi, H.-W., Bi, X.-W., Hu, R.-Z., Qi, L.-K., Yin, R.-S., et al., 2021. Mercury and sulfur isotopic composition of sulfides from sediment-hosted lead-zinc deposits in Lanping basin, Southwestern China. Chem Geol 559, 119910. https://doi.org/10.1016/j.chemgeo.2020.119910.

[48] Bergquist, B.A., Blum, J.D., 2007. Mass-dependent and-independent fractionation of Hg isotopes by photoreduction in aquatic systems. Science 318 (5849), 417–420. https://doi.org/10.1126/science.1148050.

[49] Fu, X., Zhang, H., Feng, X., Tan, Q., Ming, L., Liu, C., et al., 2019. Domestic and transboundary sources of atmospheric particulate bound mercury in remote areas of China: evidence from mercury isotopes. Environ Sci Technol 53 (4), 1947–1957. https://doi.org/10.1021/acs.est.8b06736.

[50] Sherman, L.S., Blum, J.D., Dvonch, J.T., Gratz, L.E., Landis, M.S., 2015. The use of Pb, Sr, and Hg isotopes in Great Lakes precipitation as a tool for pollution source attribution. Sci Total Environ 502, 362–374. https://doi.org/10.1016/j.scitotenv.2014.09.034.

[51] Wang, J., Dai, J., Chen, G., Jiang, F., 2022. Role of sulfur biogeochemical cycle in mercury methylation in estuarine sediments: a review. J Hazard Mater 423, 126964. https://doi.org/10.1016/j.jhazmat.2021.126964.

[52] Lin, Y., Vogt, R., Larssen, T., 2012. Environmental mercury in China: a review. Environ Toxicol Chem 31 (11), 2431–2444. https://doi.org/10.1002/etc.1980.

[53] Han, Y.-S., Kim, S.-H., Chon, C.-M., Kwon, S., Kim, J.G., Choi, H.W., et al., 2020. Effect of FeS on mercury behavior in mercury-contaminated stream sediment: a case study of Pohang Gumu Creek in South Korea. J Hazard Mater 393, 122373. https://doi.org/10.1016/j.jhazmat.2020.122373.

[54] Selin, H., Keane, S.E., Wang, S., Selin, N.E., Davis, K., Bally, D., 2018. Linking science and policy to support the implementation of the Minamata convention on mercury. Ambio 47, 198–215. https://doi.org/10.1007/s13280-017-1003-x.